Published in final edited form as:
Hum Brain Mapp. 2011 January ; 32(1): 1–9. doi:10.1002/hbm.20995.

Diffusion Tensor Imaging Reliably Differentiates Patients With Schizophrenia from Healthy Volunteers

Babak A. Ardekani, Ph.D.[1,2,*], **Ali Tabesh, Ph.D.**[1], **Serge Sevy, M.D.**[3,4,5], **Delbert G. Robinson, M.D.**[3,4,5], **Robert M. Bilder, Ph.D.**[6], and **Philip R. Szeszko, Ph.D.**[3,4,5]

[1]The Nathan S. Kline Institute for Psychiatric Research, Orangeburg, NY

[2]Department of Psychiatry, New York University School of Medicine, New York, NY

[3]Feinstein Institute for Medical Research, Manhasset, NY

[4]Zucker Hillside Hospital, Psychiatry Research, Glen Oaks, NY

[5]Albert Einstein College of Medicine, Department of Psychiatry and Behavioral Sciences, Bronx, NY

[6]UCLA Semel Institute and Geffen School of Medicine, Los Angeles, CA

Abstract

The objective of this research was to determine whether fractional anisotropy (FA) and mean diffusivity (MD) maps derived from diffusion tensor imaging (DTI) of the brain are able to reliably differentiate patients with schizophrenia from healthy volunteers. DTI and high resolution structural magnetic resonance scans were acquired in 50 patients with schizophrenia and 50 age- and sex-matched healthy volunteers. FA and MD maps were estimated from the DTI data and spatially normalized to the Montreal Neurologic Institute standard stereotactic space. Individuals were divided randomly into two groups of 50, a training set and a test set, each comprising 25 patients and 25 healthy volunteers. A pattern classifier was designed using Fisher's linear discriminant analysis based on the training set of images to categorize individuals in the test set as either patients or healthy volunteers. Using the FA maps the classifier correctly identified 94% of the cases in the test set (96% sensitivity and 92% specificity). The classifier achieved 98% accuracy (96% sensitivity and 100% specificity) when using the MD maps as inputs to distinguish schizophrenia patients from healthy volunteers in the test dataset. Utilizing FA and MD data in combination did not significantly alter the accuracy (96% sensitivity and specificity). Patterns of water self-diffusion in the brain as estimated by DTI can be used in conjunction with automated pattern recognition algorithms to reliably distinguish between patients with schizophrenia and normal control subjects.

Keywords

brain; magnetic resonance imaging; discriminant analysis; automated pattern recognition; diffusion tensor imaging; schizophrenia; mean diffusivity; fractional anisotropy

*Corresponding author: Babak A. Ardekani, Ph.D., The Nathan S. Kline Institute for Psychiatric Research, 140 Old Orangeburg Road, Orangeburg NY, 10962; phone: (845) 398 5490; fax: (845) 398 5472; ardekani@nki.rfmh.org

Introduction

Although brain abnormalities have been widely reported in patients with schizophrenia (Shenton et al. 2001), little research has been directed at determining whether this information can be used to correctly identify patients on a prospective case-by-case basis. The development of automatic pattern recognition and machine learning methods for categorizing magnetic resonance imaging (MRI) and other scans of the brain into disease and healthy classes is a relatively new and promising research area that could provide important information in this regard. Several studies used high-resolution structural MRI scans as inputs to classification algorithms to distinguish between patients with schizophrenia and healthy volunteers with reported accuracies ranging from 79% to 94% (Csernansky et al. 2004; Davatzikos et al. 2005; Fan et al., 2005; Kawasaki et al. 2007; Yoon et al. 2007). Functional MRI data have also been utilized alone or in conjunction with structural MRI information for the classification of patients and control subjects with reported accuracies in the 83% to 91% range (Ford et al. 2002; Calhoun et al. 2008; Demirci et al. 2008).

An MRI technique that may be utilized for pattern classification is diffusion tensor imaging (DTI) (Basser et al., 1994). DTI is used to characterize the magnitude and orientation of the diffusion of water molecules in the brain. The diffusion information provided by DTI at each voxel is represented by a symmetric 3×3 matrix, referred to as the diffusion tensor. Several scalar and vector quantities may be computed from the diffusion tensor at each voxel. One such measure is the fractional anisotropy (FA) which reflects the anisotropy of the self-diffusion of water molecules (Kingsley, 2006a). In white matter (WM) regions, water tends to have a higher rate of diffusion along the direction of the fibers, than perpendicular to them, because the fiber membrane and the myelin sheath present barriers to diffusion. Thus, in the WM, diffusion is normally anisotropic. The anisotropy decreases when WM fiber integrity is compromised, which results in lower FA. Growing evidence suggests that abnormalities in the white matter fiber tracts connecting different brain regions account for many clinical and cognitive manifestations of schizophrenia (Kubicki et al. 2007; Szeszko et al. 2008).

Another scalar measure derived from DTI is the mean diffusivity (MD) which reflects the magnitude of the self-diffusion of water molecules (Kingsley, 2006a). MD abnormalities have been observed in patients with schizophrenia (Ardekani et al. 2005; Lee et al. 2009; Narr et al. 2009), and likely reflect both compromised tissue integrity as well as cortical atrophy associated with the disorder.

Although abnormalities in both FA and MD measures have been identified in patients with schizophrenia compared to healthy volunteers (Ardekani et al. 2003; Ardekani et al. 2005; Kubicki et al. 2007; Lee et al. 2009; Narr et al. 2009; Szeszko et al. 2005; Szeszko et al. 2008), few studies have assessed the feasibility of using FA and/or MD maps in conjunction with automatic pattern recognition methods to differentiate between these groups. Using FA, Caan et al. (2006) reported a classification accuracy of 75% in a cohort of 34 schizophrenia patients and 24 controls estimated using five-fold cross validation, whereas Caprihan et al. (2008) achieved an 80% classification accuracy based on a leave-one-out cross validation approach in a sample of 45 patients and 45 healthy volunteers. To our knowledge, the utility of MD maps, alone or in combination with FA, to differentiate between patients with schizophrenia and healthy volunteers has not been investigated. In this study, we utilized MD and FA to distinguish between patients with schizophrenia and healthy volunteers using a linear discriminant analysis (LDA) pattern classification algorithm. This statistical approach is widely used in machine learning and uses a set of variables to identify a linear classifier that can maximally distinguish between two or more groups (Duda et al. 2001;

Mardia et al. 1979). We hypothesized that both FA and MD would reliably discriminate between patients and healthy volunteers, and that the combination of both modalities would yield an improved classification rate compared to using each modality alone.

Materials and Methods

Subjects

The fifty (34M/16F) patients with schizophrenia included in this study were recruited from inpatient and outpatient units from the Zucker Hillside Hospital in Glen Oaks, NY and had a mean age of 30.3 (SD = 10.5) years. Thirty-three patients were participating in clinical trials comparing the efficacy of antipsychotics in first-episode schizophrenia and for this study were scanned early in the course of illness (< 4.25 years from the index episode or entry into the clinical trial to the MRI). Further details regarding the ascertainment of patients and the main clinical trial from which patients were recruited are available in Robinson et al. (2006). In addition, we recruited 17 patients from the outpatient service at Zucker Hillside Hospital comprising more chronic patients who were receiving antipsychotics. Diagnoses were based on the Structured Clinical Interview for DSM-IV Axis I Disorders (SCID-I/P) (First et al. 1998) supplemented by information from family members and clinicians when available. All patients met DSM-IV criteria for schizophrenia (n = 44), schizoaffective disorder (n = 3) or schizophreniform disorder (n = 3). A total of 14 patients had the following comorbid substance abuse disorders (numbers in parentheses): alcohol abuse (10), cocaine abuse (3), cannabis abuse (3) and hallucinogen abuse (1). Of the 50 patients 8 were antipsychotic drug-naïve at the time of the scan and the rest were receiving antipsychotic medications.

In addition, fifty (34M/16F) healthy comparison subjects matched for age, sex and handedness were recruited from the community with a mean age of 31.2 (SD = 9.7) years. Exclusion criteria for healthy subjects included any Axis I psychiatric disorder (lifetime) as determined from the SCID-I/NP (First et al. 2001). Exclusion criteria for all study participants included any serious medical disorder. This study was approved by the North Shore Long Island Jewish Medical Center Institutional Review Board and written informed consent was obtained from all study participants.

Handedness

Handedness was assessed for all individuals using a modified 20-item version of the Edinburgh Inventory (Oldfield, 1971). Laterality data were missing for 1 patient and 1 healthy volunteer. A laterality quotient was computed for all individuals using the following formula: ((Total R − Total L)/(Total R + Total L) × 100), where “total R” and “total L” refer to the total number of right and left hand items scored, respectively. Scores thus ranged from +1.00 (totally dextral) to −1.00 (totally nondextral). Based on these criteria healthy volunteers had a mean (SD) laterality quotient of .72 (.58) and patients had a mean (SD) laterality quotient of .79 (.52).

Magnetic Resonance Imaging (MRI) Procedures

MR imaging exams were conducted on a GE 1.5 T system (General Electric Medical Systems, Milwaukee, WI). A total of 26 DTI volumes were obtained for each subject including 25 volumes with diffusion sensitizing gradients applied along non-parallel directions with b = 1000 s/mm^2 and two averages (NEX = 2), and one volume without diffusion weighting (b = 0; NEX = 2). Each volume consisted of 23 contiguous 5-mm axial slices acquired parallel to the anterior-posterior (AC-PC) commissural line using a ramp sampled, spin-echo, single shot echo-planar imaging (EPI) method (TR = 10 s, TE = min ms, FOV = 22 cm, matrix size = 128 × 128). A high-resolution anatomical scan with 124 contiguous coronal sections (slice thickness = 1.5 mm) was acquired covering the entire

brain using a 3D Fast SPGR sequence with IR Prep (TR = 10.1 ms, TE = 4.3 ms, TI = 600 ms, FOV = 22 cm, matrix size = 256 × 256) producing nominal in-plane resolution of 0.86 × 0.86 mm^2. In addition, an oblique axial T_2-weighted fast spin echo scan (TR = 4 s, TE = 100 ms, FOV = 22 cm, matrix size = 256 × 256, slice thickness = 5 mm, no gap) was acquired at the same slice positions and orientation as the diffusion tensor images.

Image Processing and Analysis

For all individuals, the FA and MD maps were computed from the 26 DTI volumes following estimation of a diffusion tensor at each voxel using a log-linear least squares method (Kingsley, 2006b). The FA and MD maps were obtained in the original native coordinates of the acquired images before any registration operations were applied. The FA and MD images of each subject were then transformed into standard template space. Image registration was conducted using previously published protocols (Ardekani et al. 2003; Ardekani et al. 2005; Szeszko et al. 2008). Briefly, non-brain regions were removed from the SPGR images using the Brain Extraction Tool software (Smith, 2002). Any non-brain tissue that remained following the automatic brain extraction process was removed manually using MEDx (Medical Numerics Inc., MD, USA). Using the skull-stripped SPGR, the non-brain regions were also removed from the T_2 volume after registration between the SPGR and T_2 volumes (see below). The cropped SPGR images of all subjects were spatially normalized to the Montreal Neurologic Institute's 'Colin27' MRI volume (Holmes et al. 1998) using the non-linear registration module (3dwarper) of the Automatic Registration Toolbox (ART) (Ardekani and Guckemus et al. 2005; Klein et al. 2009). For each subject, the SPGR volume was also registered to their fast spin echo T_2 volume using a rigid-body 6-parameter linear transformation obtained from ART's multimodality image registration module (Ardekani et al. 1995). To correct for the spatial distortion in the DTI EPI images, the b=0 DTI volume was registered to the skull-stripped T_2 volume using ART's distortion correction module (unwarp2d). Finally, the FA and MD volumes for each subject were transformed into the stereotactic space of the 'Colin27' template by numerically combining and applying the transformations obtained from the three registration steps outline above: (1) nonlinear within-subject mapping of the b=0 DTI volume to the skull-stripped T_2 volume for distortion correction; (2) 6-parameter linear within-subject registration of the T_2 and SPGR volumes; and (3) nonlinear between-subject mapping of the SPGR volume to the 'Colin27' reference volume. The resulting normalized FA and MD maps were used for training and classification.

Discriminant Analysis and Performance Estimation

Subjects were randomly divided into two mutually exclusive sets of fifty individuals, each comprising twenty-five patients and twenty-five healthy volunteers. The first set was used as a training set to train the classifier. The second set of images was used to evaluate the performance of the classifier. Linear discriminant analysis (LDA) was used for classification. LDA is a well-known multivariate technique (Duda et al. 2001; Mardia et al. 1979) that produces a discriminant function, or classifier, which is a linear combination of the predictor variables, in this case, voxel values in the FA or MD maps. The coefficients of the discriminant function are determined such that the ratio of the inter-class variation of the subjects in the training set to their intra-class variation is maximized. The images were rearranged into an (n × p) data matrix, where (n=50) was the number of subjects in the training set and p was the number of voxels in the skull-stripped spatially normalized FA/MD map. Specifically, the i^{th} row of this matrix contains the FA/MD map of subject i. Prior to LDA, two pre-processing steps were carried out to condition the data matrix. Both stages are linear transformations and thus can be absorbed into the LDA discriminant function to form an overall linear classifier.

In the first pre-processing stage, the voxel values at each of the p voxel locations were standardized to have zero mean and unit within-class pooled variance across subjects. Specifically, let x_{cij} denote the value of voxel j in subject i of group $c \in \{1,2\}$. The mean voxel value over all subjects (patients and controls) is given by:

$$m_j = \frac{1}{n}\left(\sum_{i=1}^{n_1} x_{1ij} + \sum_{i=1}^{n_2} x_{2ij}\right) \tag{1}$$

Where n_c denotes the number of subjects in group c ($n=n_1+n_2$). The within-class means are given by:

$$m_{cj} = \frac{1}{n_c}\sum_{i=1}^{n_c} x_{cij} \tag{2}$$

The pooled within-class sample variance is given by:

$$s_j^2 = \frac{1}{n-2}\left[\sum_{i=1}^{n_1}\left(x_{1ij} - m_{1j}\right)^2 + \sum_{i=1}^{n_2}\left(x_{2ij} - m_{2j}\right)^2\right] \tag{3}$$

The standardized voxel value is then given by:

$$y_{cij} = \frac{x_{cij} - m_j}{s_j} \tag{4}$$

If there are large within-class variations, then the sample pooled variance in (3) will be large. Then the denominator in (4) is large, which deemphasizes the data value at that particular voxel location. Note that the images $\{m_j\}$ and $\{s_j\}$ that are derived from the training data set are stored on the computer hard-disk. When a test sample is to be classified, these images are read back into memory and the standardization (4) is carried out on the test sample. Thus, the test samples undergo the exact same standardization method as the training samples.

Let Y denote the (n × p) data matrix standardized according to (4). This matrix was transformed into an n × (n−1) matrix Z using principal component analysis (PCA) given as follows:

$$\mathrm{Y} = \mathrm{U}\Lambda\mathrm{V}^{\mathrm{T}} = \mathrm{Z}\mathrm{V}^{\mathrm{T}} \tag{5}$$

As the number of voxels far exceeds the number of subjects, all of the information in the p standardized voxel values representing each subject can be summarized in the (n−1) variables contained in each row of Z. The rows of the (n−1) × p matrix V^{T} constitute a set of (n−1) orthonormal vectors that form an orthonormal basis that spans the measurement space. In effect, PCA projects the p-dimensional FA/MD maps into an (n−1)-dimensional subspace. The rows of matrix Z represent the coordinates of the maps in this subspace. Mathematically, they are computed as: Z=YV. The matrix V which is derived from the training set is stored on the computer hard-disk. When a test pattern, say p-dimensional vector a, is to be classified, the matrix V is read back into the memory and used to form the (n−1)-dimensional feature vector $b=\mathrm{V}^{\mathrm{T}}a$. The dimension of the feature vector b is then

further reduced (using the procedure described below) from (n−1) to r<(n−1) before applying using the discriminant function derived from the LDA procedure to classify the test sample.

Following PCA, the number of variables was further reduced to r<(n−1) to address the rank-deficiency of the intra-class covariance matrix. This was accomplished by removing all variables with "small" discriminative power between the patients and controls as assessed by a two-sample *t*-test. For this purpose, we eliminated all variables with *P*-values greater than 0.5. This amounted to eliminating (n−1−r) columns of the matrix Z. This resulted in an (n × r) feature matrix F. The first n_1 rows of this matrix contain the feature vectors corresponding to group 1. The remaining n_2 rows represent the feature vector for group 2. Finally LDA was performed on the data in matrix F exactly as prescribed by Mardia et al. (1979).

For a previously unseen subject, LDA produces a discriminant (abnormality) score based on their p-dimensional voxels maps. If the score is positive, the subject is assigned to one class (e.g., healthy volunteer) or, alternatively, to the other class (e.g., patient). To classify a subject on the basis of *both* FA and MD data, the abnormality scores from the two measures were used in a secondary two-dimensional LDA classifier. The accuracies of the classifiers were estimated by applying the classifier to the fifty subjects in the test set. The overall accuracy of the LDA was estimated as the proportion of correct classifications on the entire cohort. Sensitivity and specificity were measured with respect to the class of patients and healthy volunteers, respectively. The confidence interval for the classification accuracy was constructed by treating accuracy as a binomial proportion (Nadeau and Bengio, 2003). As the classification accuracy is close to 1, we obtained exact confidence intervals using the binomial distribution.

To determine whether anatomical differences between groups were evident following inter-subject registration of T_1-weighted volumes, we also trained and tested a classifier using the registered SPGR images as input patterns. Thus, in this analysis we determined sensitivity and specificity of the algorithm for categorizing patients and healthy volunteers based on their structural neuroimaging data and compared this result to that obtained using their DTI data.

Results

There were no significant group differences between patients and healthy volunteers in distributions of age, handedness or sex. The estimated accuracy of the FA-based classifier was 94% (95% CI = 83% to 99%) with 92% specificity and 96% sensitivity. The estimated classification accuracy of the MD-based classifier was 98% (95% CI = 89% to 100%) with 96% sensitivity and 100% specificity. When the FA and MD scores from the training set were used in a second level linear classifier, the estimated accuracy based on results on the test set was 96% (96% specificity and 96% sensitivity) with a 95% CI ranging from 86% to 100%.

As described previously, during the training phase, variables (principal components scores) with "small" discriminative power between patients and controls as assessed by a two-sample *t*-test were discarded. For the analysis results reported above, the number of principal components that were kept was 13 in the FA analysis and 11 in the MD analysis. This number could vary depending on the random assignment of subjects to training and test sets. In addition, to ascertain the stability of the results, we repeated the split-in-half cross validations one hundred times. The sample mean accuracy was 96.2% (SD=2.9) for the FA and 96.8% (SD=2.1) for the MD.

The discriminant scores for each of the 50 subjects in the training set are provided in Figure 1. The decision boundary for the FA-based classifier is the vertical axis and for the MD-based classifier is the horizontal axis. The boundary for the classifier that combined both FA and MD is the diagonal green line. All classifiers achieved 100% accuracy in the training set. Figure 2 illustrates the discriminant scores obtained by applying the classifier to the 50 MD and 50 FA maps from the patients and healthy volunteers in the test set. Two healthy volunteers were misclassified based on their FA maps and are represented by the two crosses to the left of the horizontal axis, which is the decision boundary of the FA-based classifier. One patient represented by a circle in the 1st quadrant was misclassified by both the FA- and MD-based LDA classifiers.

FA and MD abnormality scores of both patients and controls were strongly correlated (r = 0.93) as illustrated in Figure 2, which thus reduces the likelihood that combining the two measures would improve classification accuracy. The diagonal green line in Figure 2 illustrates the decision boundary obtained for the secondary classifier based on training data. One of the 2 control subjects in the 2nd quadrant who was misclassified based on the FA analysis was correctly classified when both the FA and MD discriminant scores obtained in the training phase were used as features in a secondary two-dimensional linear classifier. Two individuals (1 patient and 1 control) who were misclassified in the single-modality FA analysis remained misclassified in the analysis using both FA and MD.

The LDA results in a set of coefficients representing a direction in PCA space onto which the PCA space feature vector of each subject is projected to obtain their discriminant score. Each point/direction in PCA space also corresponds to an image in original image space. Thus, the coefficients of the PCA/LDA classifiers can be transformed back into image space and visualized to indicate the brain regions and the degree to which they contribute to the discrimination using the "Fisher brain." Figure 3 illustrates the Fisher brains for the FA- (a-e) and MD-based (f-j) classifiers, superimposed onto the average SPGR image of all 100 subjects in stereotactic space. In both the FA and MD images higher values in yellow regions favor classification of an individual as a healthy volunteer whereas higher values in blue regions favor classification of an individual as a patient. In general, group differences in MD appeared more pronounced in cortical and ventricular regions while FA differences included these effects as well as deep white matter regions including the bilateral external capsule.

Specificity of findings was determined by comparing the classification results obtained using the DTI data to classification of individuals using the T_1-weighted structural MR imaging data. The correct classification rate for the classifier trained using T_1-weighted structural images was only 40%, with a 95% CI ranging from 26% to 55% indicating that it performed at chance level.

Discussion

We investigated whether scalar-valued FA and MD images derived from DTI scans of the brain are able to reliably distinguish between patients with schizophrenia and healthy volunteers. A supervised pattern classifier was developed using Fisher's linear discriminant analysis based on a training set of DTI scans to prospectively categorize an independent sample of patients with schizophrenia and healthy volunteers. Classification accuracy in this independent cohort was high using either the FA- (94%) or MD images (98%); the difference in accuracy was not statistically significant, however, as evident by the overlap in their 95% confidence intervals. Additional analyses indicated that the observed findings were not significantly influenced by illness duration, diagnosis, or substance abuse. To our knowledge neither the utility of MD to differentiate patients with schizophrenia from

healthy volunteers nor whether the combination of MD and FA yields improved classification compared to either modality alone has been investigated. It is noteworthy that the algorithm performed at chance level when structural magnetic resonance images were used for classification suggesting that the inter-subject registration method had successfully removed major shape differences between the subjects' brain.

Few studies have attempted to discriminate between patients with schizophrenia and healthy volunteers using DTI and automatic pattern recognition methods. Two recent studies, however, examined the utility of FA to distinguish between patients with schizophrenia compared to healthy volunteers (Caan et al. 2006, Caprihan et al. 2008) with reported accuracies ranging from 75% using five-fold cross validation (Caan et al. 2006) to 80% using leave one out cross validation (Caprihan et al. 2008). Our data suggest that higher classification using FA, and additionally, MD may be possible compared to prior investigations. The improved accuracy in the current study may be related to our use of a relatively large cohort, the use of well-standardized diagnostic instruments for assessing both patients and healthy volunteers and particularly the inter-subject registration algorithm used in the present investigation, which has been demonstrated empirically to be more accurate compared to many other currently available methods (Ardekani and Guckemus et al. 2005; Klein et al. 2009). In particular, the accuracy and quality of the registration algorithm (an illustration of the average of 100 registered SPGR images in our study is provided in Figure 3) is a critical component in image-based classification and likely to contribute significantly to study results.

It should be emphasized that the current study was carefully designed to avoid the typical pitfalls in prediction studies. As discussed by Demirci et al. (2008), four common problems may bias the results of prediction studies: a small cohort that may not be representative of the populations of interest; presenting only the overall prediction accuracy potentially concealing low classification accuracies for classes having fewer subjects; using the full set of subjects for any stage of feature/classifier selection; and reporting the cross validation accuracy for the optimized classifier obtained with the same cross validation. To the best of our knowledge, the sample size in our study is among the largest reported in the literature on the classification of patients with schizophrenia and healthy controls. We have reported both the sensitivity and specificity to characterize the classification performance on both patient and control groups. We have also carefully separated the steps in training and testing the classifiers to avoid the last two sources of bias described above. The steps of standardization, PCA, and principal component selection, and training the LDA were all carried out using the training set, and then the final optimized classifier was applied to classify the previously unseen test subjects. As noted in the Methods section, PCA projects the p-dimensional (FA/MD) maps into an $(n–1)$-dimensional subspace. Following PCA, the number of variables may be further reduced by removing those elements of the $(n–1)$-dimensional feature vectors with small discriminative power between the patients and controls. In the present paper, we assess discriminative power by a two-sample t-test. That is, we eliminate all variables with P-values greater than some threshold. Caprihan et al. (2008) utilized a similar approach in which the "discriminative power" of variables is assessed based on the Mahalanobis distance between groups.

When the normalized T_1-weighted images were used as inputs to the classification algorithm, the classifier performed at chance level. This is an indication that the spatial normalization technique (ART) used in this study was effective in removing systematic anatomical differences between patients and controls. It should be mentioned that higher classification accuracies (81% to 91%) have been reported in the literature when using purely structural scans as basis for classification (Davatzikos et al. 2005; Fan et al., 2005; Kawasaki et al. 2007). It should be pointed out, however, that in those studies the feature

vectors used for classification were gray matter density maps computed using methods similar to the voxel-based morphometry technique (Good et al. 2001), and thus our structural imaging results may not be directly comparable to prior investigations.

Brain regions that distinguished between patients and healthy volunteers are provided in the Fisher brains in Figure 3. The Fisher brains were thresholded such that voxels with an absolute value greater than 30% of the maximum absolute voxel value are illustrated to avoid clutter when visualizing the brain regions that contributed to the classification. Brain regions that contributed to the group classification were mostly symmetric for both FA and MD and were evident in both cortical, white matter and ventricular regions. While MD effects were most evident in cortical and ventricular regions FA effects included these effects and, in addition, deep white matter regions such as the external capsule. Group differences were also observed near the border between the brain and cerebrospinal fluid near the edge of the ventricles and thus, our approach may be sensitive to group differences in water diffusion properties in these regions. Brain regions that contributed to the high classification rate using the DTI scans were not simply a function of possible ventricular enlargement in patients, however, given that group differences in white matter also contributed to the classification and most importantly, group classification based on the structural magnetic resonance images performed only at chance level.

While the classical PCA/LDA algorithm produces robust classifiers as evidenced by the high classification accuracy observed in this study, recent advances in machine learning have led to the development of additional algorithms for pattern representation and classification. Thus, it would be important to evaluate other feature extraction/selection methods in conjunction with state-of-the-art classifiers, including support vector machines (De Martino et al., 2008; Gerardin et al. 2009; Sato et al. 2008). Moreover, it would be worthwhile to determine whether a classifier trained on DTI data from one center could be used to reliably classify scans obtained from another center. In this regard, FA may be a more suitable scalar measure as it has a natural scaling that may be useful for pooling data across centers.

Although the observed effects were identified in a cohort of patients where the diagnosis of schizophrenia was already established an important extension of this work is the identification of individuals at high risk for developing psychosis as anatomical changes in such patients may be observed at a young age (Gogtay et al., 2008; Thompson et al. 2001; Vidal et al. 2006). In this regard Koutsouleris and colleagues (Koutsouleris et al. 2009) used support vector machines to correctly identify individuals who were in “at risk mental states of psychosis” as well as those individuals who transitioned into psychosis. Another valuable extension of this work would be to determine whether such classification methods distinguish among individuals with different psychiatric disorders, although this may be inherently more complex as some research suggests that some disorders such as schizophrenia and bipolar disorder share common structural alterations (Sussmann et al. 2009; McIntosh et al. 2004).

There were several study limitations that should be acknowledged. One limitation of the classification approach is that it does readily lend itself to localizing group differences in specific regions. The methodology presented here, however, may be used as a starting point for this purpose using randomization methods (Ardekani et al. 1998). An additional study limitation is the anisotropic voxel size, which could conceivably bias FA measurements, although it should be noted these were comparable in both groups. In addition, the DTI images were acquired with NEX=2, which does not always allow for identification of artifacts especially those from cardiac pulsation. Additionally, patients tend to have lower IQs compared to healthy volunteers, and given evidence that IQ and cognitive abilities

correlate with FA and MD (Fryer et al. 2008, Schmithorst et al. 2005) an additional possible study limitation is that the discriminant function may be sensitive to generalized brain abnormalities, such as those that may be indexed by IQ, and thus not actually be specific to schizophrenia *per se*. Moreover, we were unable to examine other possible factors that could influence brain measurements such as nutrition or antipsychotic medication and the functional significance of the classification methodology was not investigated.

Conclusion

This study demonstrated the utility of using FA and MD to distinguish between patients with schizophrenia and healthy volunteers. Using LDA, we achieved accuracies of 94% and 98% for FA and MD, respectively, in a test cohort of 25 patients and 25 healthy volunteers. Combining the information from FA and MD, however, did not improve the classification accuracy due to the high degree of correlation between these measures. Scalar-valued measures, FA and MD, derived from DTI, which characterize the diffusion of water molecules in the brain can be used in conjunction with pattern recognition and machine learning methods to accurately distinguish between patients with schizophrenia and healthy volunteers.

Acknowledgments

This work was supported in part by grants from NARSAD (PRS) and the National Institute of Mental Health to Dr. Szeszko (MH01990; MH76995), Dr. Robinson (MH60004), Dr. Bilder (MH60374), the Zucker Hillside Center for Intervention Research in Schizophrenia (P30 MH060575), the NSLIJ Research Institute General Clinical Research Center (M01 RR018535), and grants from the National Institute of Biomedical Imaging and Bioengineering and the National Institute of Neurological Disorders and Stroke (R03EB8201) to Dr. Ardekani.

References

Ardekani BA, Bappal A, D'Angelo D, Ashtari M, Lencz T, Szeszko PR, Butler PD, Javitt DC, Lim KO, Hrabe J, Nierenberg J, Branch CA, Hoptman MJ. Brain morphometry using diffusion-weighted magnetic resonance imaging: application to schizophrenia. Neuroreport 2005;16:1455–1459. [PubMed: 16110271]

Ardekani BA, Braun M, Hutton BF, Kanno I, Iida H. A fully automatic multimodality image registration algorithm. J Comput Assist Tomogr 1995;19:615–623. [PubMed: 7622696]

Ardekani BA, Guckemus S, Bachman A, Hoptman MJ, Wojtaszek M, Nierenberg J. Quantitative comparison of algorithms for inter-subject registration of 3D volumetric brain MRI scans. J Neurosci Methods 2005;142:67–76. [PubMed: 15652618]

Ardekani BA, Nierenberg J, Hoptman MJ, Javitt DC, Lim KO. MRI study of white matter diffusion anisotropy in schizophrenia. Neuroreport 2003;14:2025–2029. 2003. [PubMed: 14600491]

Ardekani, BA.; Strother, SC.; Anderson, JR.; Law, I.; Paulson, OB.; Kanno, I.; Rottenberg, DA. On the detection of activation patterns using principal components analysis. In: Carson, RE.; Daube-Witherspoon, ME.; Herscovitch, P., editors. Quantitative functional brain imaging with positron emission tomography. Academic; San Diego: 1998. p. 253-237.

Caan MWA, Vermeer KA, van Vliet LJ, Majoie CBLM, Peters BD, den Heeten GJ, Vos FM. Shaving diffusion tensor images in discriminant analysis: a study into schizophrenia. Med Image Anal 2006;10:841–849. [PubMed: 16965928]

Calhoun VD, Maciejewski PK, Pearlson GD, Kiehl KA. Temporal lobe and "default" hemodynamic brain modes discriminate between schizophrenia and bipolar disorder. Human Brain Mapping 2008;29:1265–75. [PubMed: 17894392]

Caprihan A, Pearlson GD, Calhoun VD. Application of principal component analysis to distinguish patients with schizophrenia from healthy controls based on fractional anisotropy measurements. Neuroimage 2008;42:675–682. [PubMed: 18571937]

Csernansky JG, Schindler MK, Splinter NR, Wang L, Gado M, Selemon LD, Rastogi-Cruz D, Posener JA, Thompson PA, Miller MI. Abnormalities of thalamic volume and shape in schizophrenia. Am J Psychiatry 2004;161:896–902. [PubMed: 15121656]

Davatzikos C, Shen D, Gur RC, Wu X, Liu D, Fan Y, Hughett P, Turetsky BI, Gur RE. Whole-brain morphometric study of schizophrenia revealing a spatially complex set of focal abnormalities. Arch Gen Psychiatry 2005;62:1218–1227. [PubMed: 16275809]

Demirci O, Clark VP, Magnotta VA, Andreasen NC, Lauriello J, Kiehl KA, Pearlson GD, Calhoun VD. A review of challenges in the use of fMRI for disease classification / characterization and a projection pursuit application from multi-site fMRI schizophrenia study. Brain Imaging Behav 2008;2:147–226. [PubMed: 19562043]

De Martino F, Valente G, Staeren N, Ashburner J, Goebel R, Formisano E. Combining multivariate voxel selection and support vector machines for mapping and classification of fMRI spatial patterns. Neuroimage 2008;43:44–58. [PubMed: 18672070]

Duda, R.; Hart, P.; Stork, D. Pattern Classification. Wiley; New York: 2001.

Fan Y, Shen D, Davatzikos C. Classification of structural images via high-dimensional image warping, robust feature extraction, and SVM. Med Image Comput Comput Assist Interv Int Conf Med Image Comput Comput Assist Interv 2005;8:1–8.

First, MB.; Spitzer, RL.; Gibbon, M.; Williams, JBW. Structured Clinical Interview for DSM-IV Axis-I Disorders - Patient Edition (SCID-I/P, Version 2.0, 8/98 revision). Biometrics Research Department, New York State Psychiatric Institute; New York: 1998.

First, MB.; Spitzer, RL.; Gibbon, M.; Williams, JBW. Structured Clinical Interview for DSM-IV-TR Axis I Disorders - Non-patient Edition (SCID-I/NP, 2/2001 revision). Biometrics Research Department, New York State Psychiatric Institute; New York: 2001.

Ford, J.; Shen, L.; Makedon, F.; Flashman, LA.; Saykin, AJ. A combined structural-functional classification of schizophrenia using hippocampal volume plus fMRI activation; Second Joint EMBS/BMES Conference; Houston, TX. 2002;

Fryer SL, Frank LR, Spadoni AD, Theilmann RJ, Nagel BJ, Schweinsburg AD, Tapert SF. Microstructural integrity of the corpus callosum linked with neuropsychological performance in adolescents. Brain Cogn 2008;67:225–33. [PubMed: 18346830]

Gerardin E, Chételat G, Chupin M, Cuingnet R, Desgranges B, Kim HS, Niethammer M, Dubois B, Lehéricy S, Garnero L, Eustache F, Colliot O. Multidimensional classification of hippocampal shape features discriminates alzheimer's disease and mild cognitive impairment from normal aging. The alzheimer's disease neuroimaging initiative. Neuroimage. 2009 in press.

Gogtay N, Lu A, Leow AD, Klunder AD, Lee AD, Chavez A, Greenstein D, Giedd JN, Toga AW, Rapoport JL, Thompson PM. Three-dimensional brain growth abnormalities in childhood-onset schizophrenia visualized by using tensor-based morphometry. Proc Natl Acad Sci USA 2008;105:15979–15984. [PubMed: 18852461]

Good CD, Johnsrude IS, Ashburner J, Henson RN, Friston KJ, Frackowiak RS. A voxel-based morphometric study of ageing in 465 normal adult human brains. Neuroimage 2001;14:21–36. [PubMed: 11525331]

Holmes CJ, Hoge R, Collins L, Woods R, Toga AW, Evans AC. Enhancement of MR images using registration for signal averaging. J Comput Assist Tomogr 1998;22:324–333. [PubMed: 9530404]

Kawasaki Y, Suzuki M, Kherif F, Takahashi T, Zhou SY, Nakamura K, Matsui M, Sumiyoshi T, Seto H, Kurachi M. Multivariate voxel-based morphometry successfully differentiates schizophrenia patients from healthy controls. Neuroimage 2007;34:235–242. [PubMed: 17045492]

Kingsley PB. Part II. Anisotropy, diffusion-weighting factors, and gradient encoding schemes. Concepts in Mag Res A 2006a;28A:123–154. Introduction to diffusion tensor imaging mathematics.

Kingsley PB. Part III. Tensor calculation, noise, simulations, and optimization. Concepts in Mag Res A 2006b;28A:155–179. Introduction to diffusion tensor imaging mathematics.

Klein A, Andersson J, Ardekani BA, Ashburner J, Avants B, Chiang MC, Christensen GE, Collins DL, Gee J, Hellier P, Song JH, Jenkinson M, Lepage C, Rueckert D, Thompson P, Vercauteren T, Woods RP, Mann JJ, Parsey RV. Evaluation of 14 nonlinear deformation algorithms applied to human brain MRI registration. Neuroimage 2009;46:786–802. [PubMed: 19195496]

Koutsouleris N, Meisenzahl EM, Davatzikos C, Bottlender R, Frodi T, Scheuerecker J, Schmitt G, Zetzsche T, Decker P, Reiser M, Moller HJ, Gaser C. Use of neuroanatomical pattern classification to identify subjects in at-risk mental states of psychosis and predict disease transition. Arch Gen Psychiatry 2009;66:700–712. [PubMed: 19581561]

Kubicki M, McCarley R, Westin CF, Park HJ, Maier S, Kikinis R, Jolesz FA, Shenton ME. A review of diffusion tensor imaging studies in schizophrenia. J Psychiatr Res 2007;41:15–30. [PubMed: 16023676]

Lee K, Yoshida T, Kubicki M, Bouix S, Westin CF, Kindlmann G, Niznikiewicz M, Cohen A, McCarley RW, Shenton ME. Increased diffusivity in superior temporal gyrus in patients with schizophrenia: a Diffusion Tensor Imaging study. Schizophr Res 2009;113:109–10. [PubMed: 19559570]

Mardia, KV.; Kent, JT.; Bibby, JM. Multivariate Analysis. Academic Press; San Diego: 1979.

McIntosh AM, Job DE, Moorhead TW, Harrison LK, Forrester K, Lawrie SM, Johnstone EC. Voxel-based morphometry of patients with schizophrenia or bipolar disorder and their unaffected relatives. Biol Psychiatry 2004;56:544–52. [PubMed: 15476683]

Nadeau C, Bengio Y. Inference for the generalization error. J Mach Learn Res 2003;52:239–281.

Narr KL, Hageman N, Woods RP, Hamilton LS, Clark K, Phillips O, Shattuck DW, Asarnow RF, Toga AW, Nuechterlein KH. Mean diffusivity: a biomarker for CSF related disease and genetic liability effects in schizophrenia. Psychiatry Res 2009;171:20–32. [PubMed: 19081707]

Oldfield RC. The assessment and analysis of handedness: the Edinburgh inventory. Neuropsychologia 1971;9:97–113. [PubMed: 5146491]

Robinson DG, Woerner MG, Napolitano B, Patel RC, Sevy SM, Gunduz-Bruce H, et al. Randomized comparison of olanzapine versus risperidone for the treatment of first-episode schizophrenia: 4-month outcomes. Am J Psychiatry 2006;163:2096–2102. [PubMed: 17151160]

Sato JR, Mourão-Miranda J, Morais Martin Mda G, Amaro E Jr, Morettin PA, Brammer MJ. The impact of functional connectivity changes on support vector machines mapping of fMRI data. J Neurosci Methods 2008;172:94–104. [PubMed: 18499266]

Schmithorst VJ, Wilke M, Dardzinski BJ, Holland SK. Cognitive functions correlate with white matter architecture in a normal pediatric population: a diffusion tensor MRI study. Hum Brain Map 2005;26:139–47.

Shenton ME, Dickey CC, Frumin M, McCarley RW. A review of MRI findings in schizophrenia. Schizophr Res 2001;49:1–52. [PubMed: 11343862]

Smith SM. Fast robust automated brain extraction. Hum Brain Mapp 2002;17:143–155. [PubMed: 12391568]

Sussmann JE, Lymer GK, McKirdy J, Moorhead TW, Maniega SM, Job D, Hall J, Bastin ME, Johnstone EC, Lawrie SM, McIntosh AM. White matter abnormalities in bipolar disorder and schizophrenia detected using diffusion tensor magnetic resonance imaging. Bipolar Disord 2009;11:11–18. [PubMed: 19133962]

Szeszko PR, Ardekani BA, Ashtari M, Kumra S, Robinson DG, Sevy S, Gunduz-Bruce H, Malhotra AK, Kane JM, Bilder RM, Lim KO. White matter abnormalities in first-episode schizophrenia or schizoaffective disorder: a diffusion tensor imaging study. Am J Psychiatry 2005;162:602–605. [PubMed: 15741480]

Szeszko PR, Robinson DG, Ashtari M, Vogel J, Betensky J, Sevy S, Ardekani BA, Lencz T, Malhotra AK, McCormack J, Miller R, Lim KO, Gunduz-Bruce H, Kane JM, Bilder RM. Clinical and neuropsychological correlates of white matter abnormalities in recent onset schizophrenia. Neuropsychopharmacology 2008;33:976–984. [PubMed: 17581532]

Thompson PM, Vidal C, Giedd JN, Gochman P, Blumenthal J, Nicolson R, Toga AW, Rapoport JL. Mapping adolescent brain change reveals dynamic wave of accelerated gray matter loss in very early-onset schizophrenia. Proc Natl Acad Sci USA 2001;98:11650–11655. [PubMed: 11573002]

Vidal CN, Rapoport JL, Hayashi KM, Geaga JA, Sui Y, McLemore LE, Alaghband Y, Giedd JN, Gochman P, Blumenthal J, Gogtay N, Nicolson R, Toga AW, Thompson PM. Dynamically spreading frontal and cingulate deficits mapped in adolescents with schizophrenia. Arch Gen Psychiatry 2006;63:25–34. [PubMed: 16389194]

Yoon U, Lee JM, Im K, Shin YW, Cho BH, Kim IY, Kwon JS, Kim SI. Pattern classification using principal components of cortical thickness and its discriminative pattern in schizophrenia. NeuroImage 2007;34:1405–15. [PubMed: 17188902]

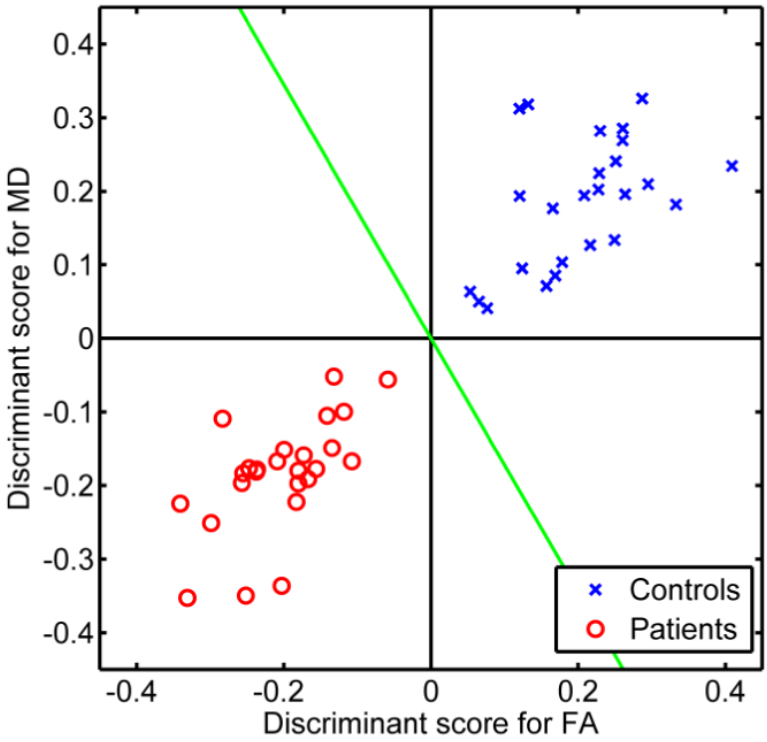

Figure 1.
Scatter plot of FA and MD discriminant scores for the 50 training subjects. The vertical axis is the decision boundary for the FA score. The horizontal axis is the decision boundary of the MD score. There green diagonal axis is the decision boundary of the second level linear classifier that combines the FA and MD scores.

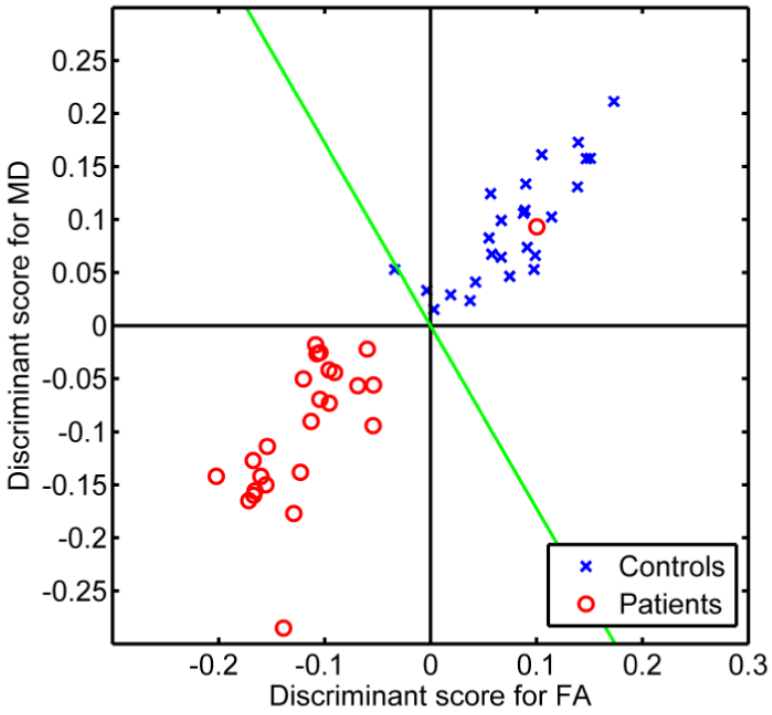

Figure 2.

Scatter plot of FA and MD discriminant scores for the 50 test subjects. The decision boundaries are the same as in Figure 1. One patient (circle in first quadrant) is misclassified based on both their FA and MD features. Two healthy volunteers (crosses in the second quadrant) and misclassified based on their FA but not MD. When the bimodal classifier is used, one of the two healthy volunteers is classified correctly (represented by the cross in the second quadrant to the right of the green diagonal line).

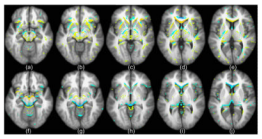

Figure 3.
Selected slices from the FA (a-e) and MD (f-j) “Fisher brains” superimposed on the average SPGR images of all subjects. From left to right, the axial slices represent sections −10, −5, 0, 5, and 10 mm above the AC-PC plane. The Fisher brains are thresholded at 30% of their maximum absolute value. In both the FA and MD images higher values in yellow regions favor classification of an individual as a healthy volunteer whereas higher values in blue regions favor classification of an individual as a patient.